

Oral micro-to-nano genome-editing system enabling targeted delivery and conditional activation of CRISPR-Cas9 for gene therapy of inflammatory bowel disease

Sicen Lin^{1,#}, Shuwen Han^{2,#}, Xu Wang¹, Xinyue Wang¹, Xianbao Shi³, Zhonggui He^{1,5}, Mengchi Sun^{4,5,} and Jin Sun^{1,5,*}*

¹Wuya College of Innovation, Shenyang Pharmaceutical University, Shenyang 110016, Liaoning, China

²Huzhou Central Hospital, Affiliated Central Hospital Huzhou University, Huzhou 313000, Zhejiang, China

³Department of Pharmacy, The First Affiliated Hospital of Jinzhou Medical University, Jinzhou 121001, Liaoning, China

⁴School of Pharmacy, Shenyang Pharmaceutical University, Shenyang 110016, Liaoning, China

⁵Joint International Research Laboratory of Intelligent Drug Delivery Systems, Ministry of Education, Shenyang 110016, Liaoning, China

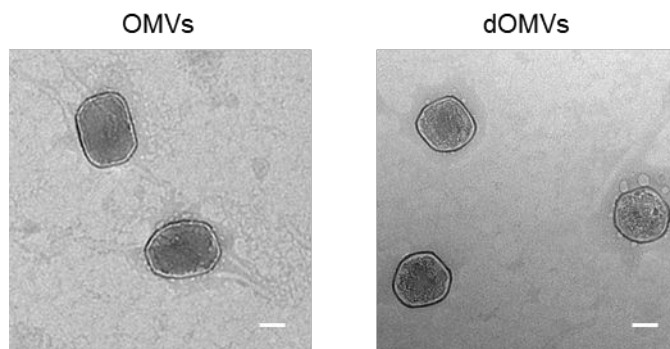


Figure S1. Representative TEM images of OMVs and dOMVs. Scale bar, 50 nm.

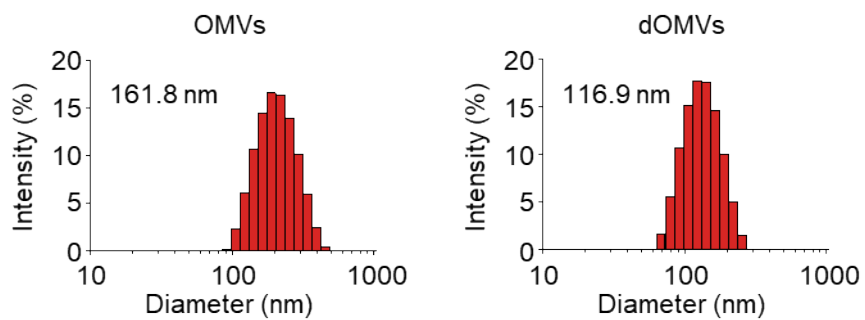


Figure S2. Size distribution of OMVs and dOMVs.

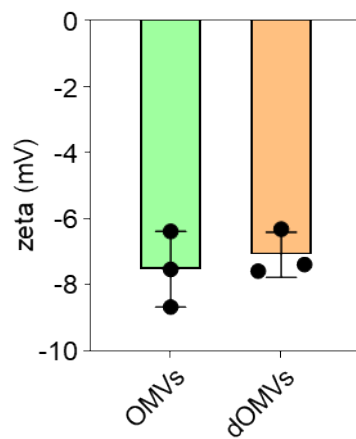


Figure S3. Zeta potential analysis of OMVs and dOMVs. Data are presented as mean \pm SD ($n=3$).

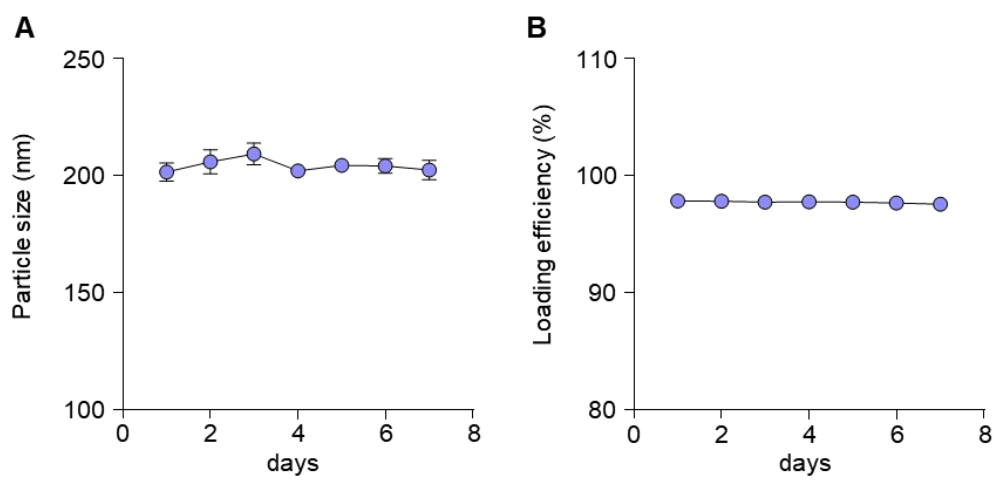


Figure S4. The particle size (A) and encapsulation efficiency (B) of RNP-NCs@dOMV stored in PBS (pH 7.4) at 4°C for 7 days ($n=3$).

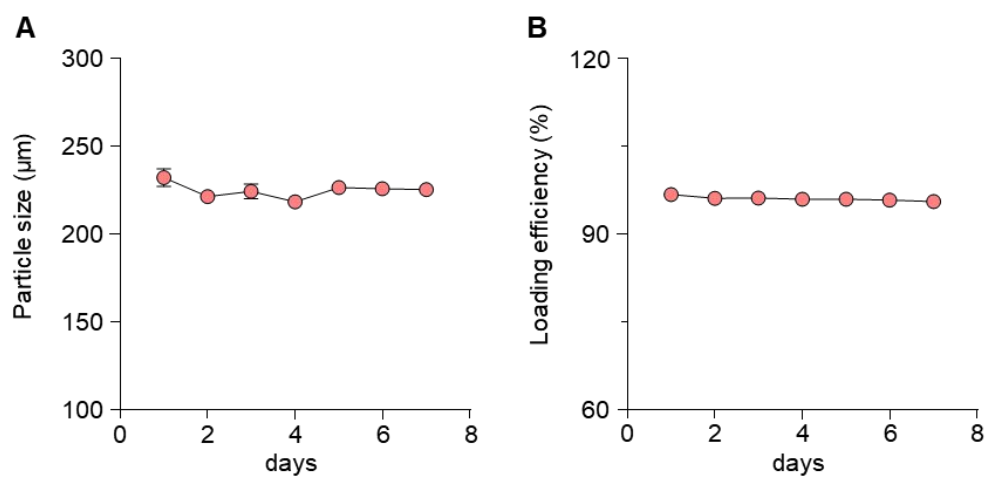


Figure S5. The particle size (A) and encapsulation efficiency (B) of RNP-NCs@dOMV@CAM stored in CaCl₂ solution at 4°C for 7 days ($n=3$).

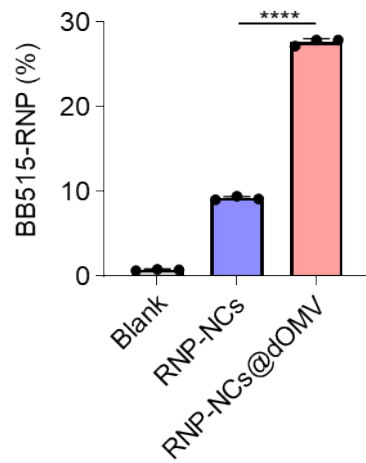


Figure S6. The cellular interaction of RNP-NCs and RNP-NCs@dOMV by flow cytometric analyses ($n=3$). Data are presented as mean \pm SD, ns: no significance, * $p<0.05$, ** $p<0.01$, *** $p<0.001$ and **** $p<0.0001$ calculated using two-tailed Student's test.

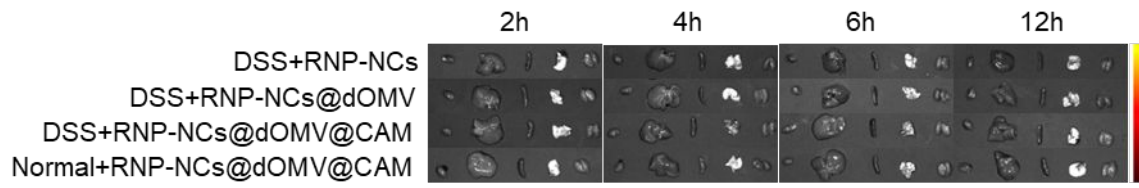


Figure S7. *Ex vivo* IVIS imaging of major organs from IBD mice and healthy mice receiving specified treatments.

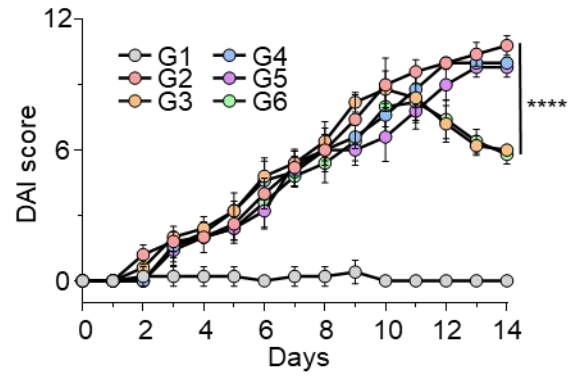


Figure S8. Daily disease activity index (DAI) scores in different treatment groups ($n=4$). G1: Normal, G2: DSS, G3: DSS+5-ASA, G4: DSS+dOMVs, G5: DSS+RNP-NCs@dOMV, G6: DSS+RNP-NCs@dOMV@CAM. Data are presented as mean \pm SD, ns: no significance, $*p<0.05$, $**p<0.01$, $***p<0.001$ and $****p<0.0001$ calculated using two-tailed Student's test.

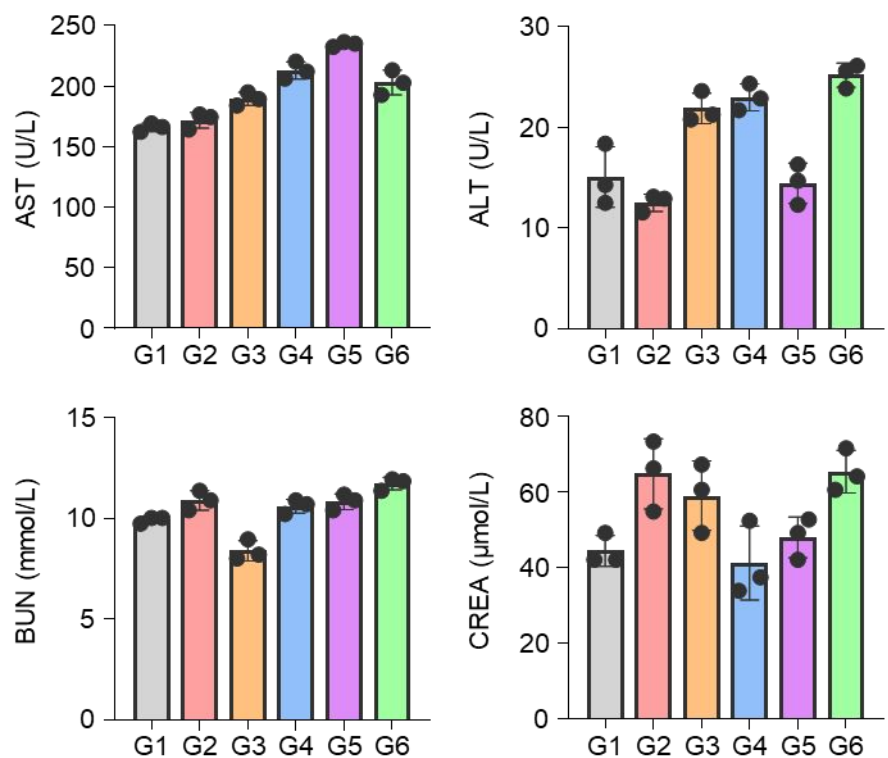


Figure S9. Measurement of liver and kidney function parameters, including aspartate aminotransferase (AST), alanine aminotransferase (ALT), creatinine (CREA), and blood urea nitrogen (BUN) levels ($n=3$). G1: Normal, G2: DSS, G3: DSS+5-ASA, G4: DSS+dOMVs, G5: DSS+RNP-NCs@dOMV, G6: DSS+RNP-NCs@dOMV@CAM. Data are presented as mean \pm SD.

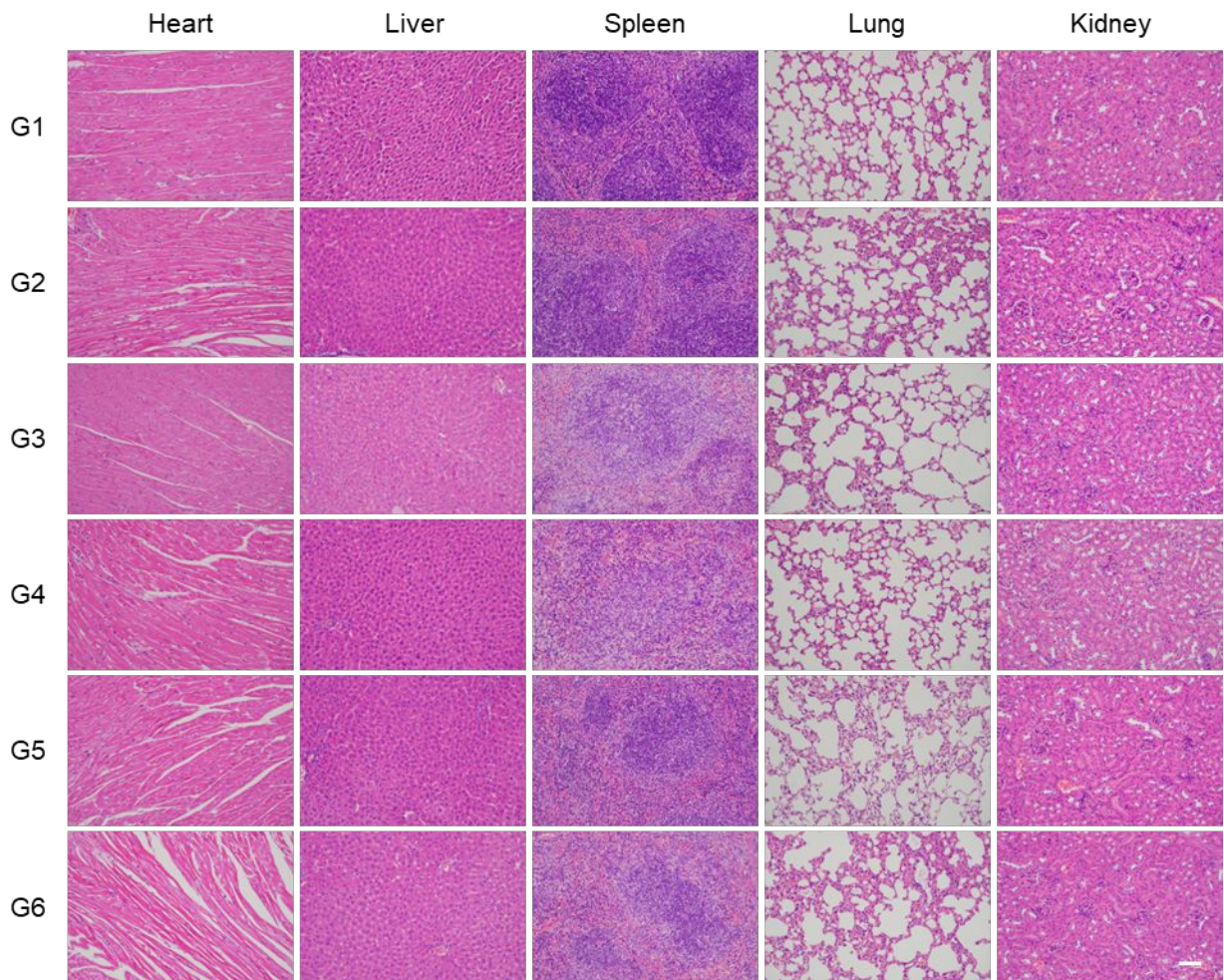


Figure S10. Sections of major organs (heart, liver, spleen, lungs, kidneys) stained with hematoxylin and eosin (H&E) were analyzed for systemic toxicity. Scale bar, 200 μ m. G1: Normal, G2: DSS, G3: DSS+5-ASA, G4: DSS+dOMVs, G5: DSS+RNP-NCs@dOMV, G6: DSS+RNP-NCs@dOMV@CAM.

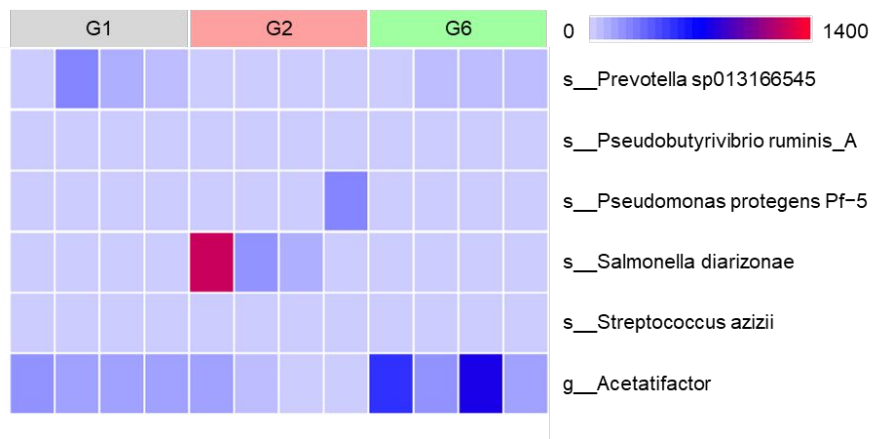


Figure S11. Heatmap exhibited the relative abundance of microbial compositional profiling at a specie level. Each column represents each mouse ($n=4$). G1: Normal, G2: DSS, G6: DSS+RNP-NCs@dOMV@CAM.

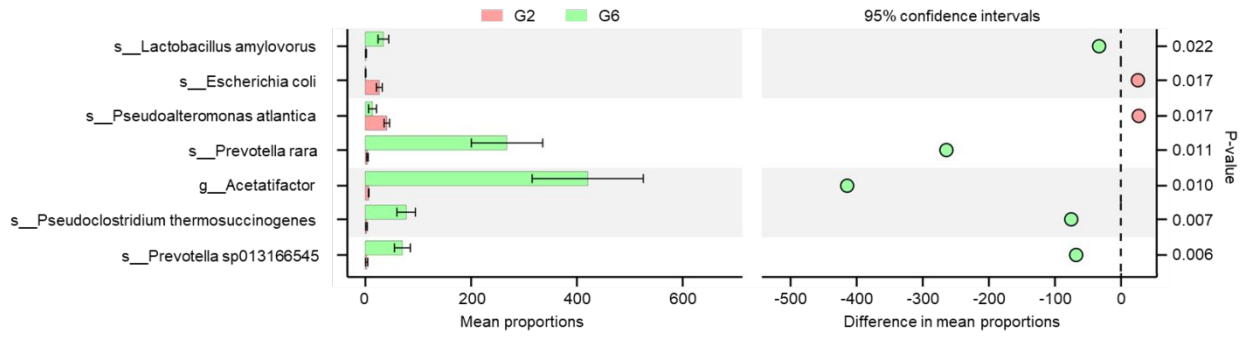


Figure S12. Analysis of species with significant differences using the t-test ($n=4$). G2: DSS, G6: DSS+RNP-NCs@dOMV@CAM.

sgRNA name	Sequences (5'-3')
sgRNA-1	AAGAAAUCUUACCUACGACGGUUUUAGAGCUAGAAA UAGCAAGUUAAAAUAAGGCUAGUCCGUUAUCAACUU GAAAAGUGGCACCGAGUCGGUGCUUUU
sgRNA-2	GUAGACAAGGUACAACCCAUGUUUUAGAGCUAGAAA UAGCAAGUUAAAAUAAGGCUAGUCCGUUAUCAACUU GAAAAGUGGCACCGAGUCGGUGCUUUU
sgRNA-3	UGGGCCAUAGAACUGAUGAGGUUUUAGAGCUAGAAA UAGCAAGUUAAAAUAAGGCUAGUCCGUUAUCAACUU GAAAAGUGGCACCGAGUCGGUGCUUUU

Table S1. Sequences of sgRNA used in this study.